Traffic Flow Theory and Car Following

Nonstationary Kalman Filter for Estimation of Accurate and Consistent Car-Following Data

Vincenzo Punzo, Domenico Josto Formisano, and Vincenzo Torrieri

Difficulty in obtaining accurate car-following data has traditionally been regarded as a considerable drawback in understanding real phenomena and has affected the development and validation of traffic microsimulation models. Recent advancements in digital technology have opened up new horizons in the conduct of research in this field. Despite the high degrees of precision of these techniques, estimation of time series data of speeds and accelerations from positions with the required accuracy is still a demanding task. The core of the problem is filtering the noisy trajectory data for each vehicle without altering platoon data consistency; i.e., the speeds and accelerations of following vehicles must be estimated so that the resulting intervehicle spacings are equal to the real one. Otherwise, negative spacings can also easily occur. The task was achieved in this study by considering vehicles of a platoon as a sole dynamic system and reducing several estimation problems to a single consistent one. This process was accomplished by means of a nonstationary Kalman filter that used measurements and time-varying error information from differential Global Positioning System devices. The Kalman filter was fruitfully applied here to estimation of the speed of the whole platoon by including intervehicle spacings as additional measurements (assumed to be reference measurements). The closed solution of an optimization problem that ensures strict observation of the true intervehicle spacings concludes the estimation process. The stationary counterpart of the devised filter is suitable for application to position data, regardless of the data collection technique used, e.g., video cameras.

The use of microscopic traffic flow models to evaluate complex real contexts, such as the implementation of intelligent transportation system strategies on congested road networks, has proved how inappropriate such models are in accurately representing the real world. One of the major reasons has been long identified from the inadequacy of their submodels, including car-following ones.

Although most of the car-following submodels are still used, they were developed after the historic study performed by the group of General Motors researchers (1) between the mid-1950s and the 1970s and after some valuable contributions from other investigators (2, 3). Starting from some simple assumptions, they were developed through a fundamentally deductive approach. Major efforts have been devoted to the study of the theoretical properties of models, such as stability. By contrast, empirical verification of the assumptions and model calibration have encountered serious difficulties with the collection of accurate, unbiased data. Major technological issues arise in the collection of time series data of vehicle motion variables with high degrees of accuracy and in a common space–time reference system. For this reason, too, findings from calibration studies have often been contradictory [for a comprehensive review, see the work of Brackstone and McDonald (4)].

As the collection of accurate experimental data could substantially improve the knowledge of real phenomena and the realism of models, the recent development of digital technology has opened up new horizons in the conduct of research in this field. Experiments with several techniques for gathering vehicle trajectories have been conducted (see the next section).

However, whatever approach is used and despite the high expected degree of precision of instruments, the estimation of trajectories from raw data is a demanding task. The requirements for the effective use of such data in car-following studies are indeed stringent. Estimated speed and acceleration time series must be free of noise. That is, they must respect physical limitations and they must be smoothed. Moreover, they must be consistent: the speeds and accelerations of following vehicles must be estimated in such a way that the resulting intervehicle spacings are equal to real spacings. Otherwise, for example, even slight differences between the estimated and the actual speeds of a vehicle may easily entail negative spacings in the case of a stop (i.e., in cases in which the actual spacings are very small; see the next section for an example).

To the authors' knowledge, despite its importance, this consistency requirement for estimated data has not been explicitly stressed in previous work. Raw data collected from different vehicles are generally processed independently, i.e., without the imposition of any consistency condition (5, 6).

To address this problem, following vehicles can instead be considered a sole dynamic system and one consistent estimation problem instead of several independent ones can be solved. The Kalman filter is a suitable device for such a task (7). It allows the system of n vehicles to be represented with a state–space model and estimation of state variable values (vehicle cinematic variables) as the best compromise between measurements and model estimates.

The structure of the filter presented below is suitable for estimation of time series data of speeds (and accelerations) from vehicle positions with whatever technology with which the data are collected. If time-varying estimates of measurement errors are available, as in the case of a differential Global Positioning System (GPS), a nonstationary filter can be devised. Otherwise, as with data from video cameras, a stationary filter is valid.

In this paper, the data requirements for car-following studies, the available collection techniques, and the experiments carried out for this work are briefly discussed first. The available information from GPS

devices and the different estimation techniques compared in this work are then presented. The structure and properties of the nonstationary Kalman filter that was devised and a further refinement to the estimation process follow. The paper concludes with a comparison of the performances of the different estimation techniques tested.

CAR-FOLLOWING DATA

Requirements of Experimental Data

The data required for car-following studies consist of the space–time trajectories of vehicles, that is, the availability of vehicle positions over time in an absolute space–time reference system (e.g., from data

from video cameras or onboard GPS receivers; see below). From these positional data, time series of intervehicle spacings are immediately available, while vehicle speeds and accelerations must be calculated through successive derivations of the space traveled.

As raw position data are subject to measurement errors, the latter are amplified in the derivation process (see Figure 1 for an example). The resulting speeds and accelerations can present physically incompatible values. Moreover, their temporal profiles can be very noisy. Such deviations can significantly affect both car-following behavior analysis and the estimation of model parameters through a direct method, e.g., maximum-likelihood methods [an application has been provided elsewhere (5)]. On the other hand, when noisy time series of speeds or accelerations are used to feed models in an iterative calibration process [i.e., through an indirect method, such as that used
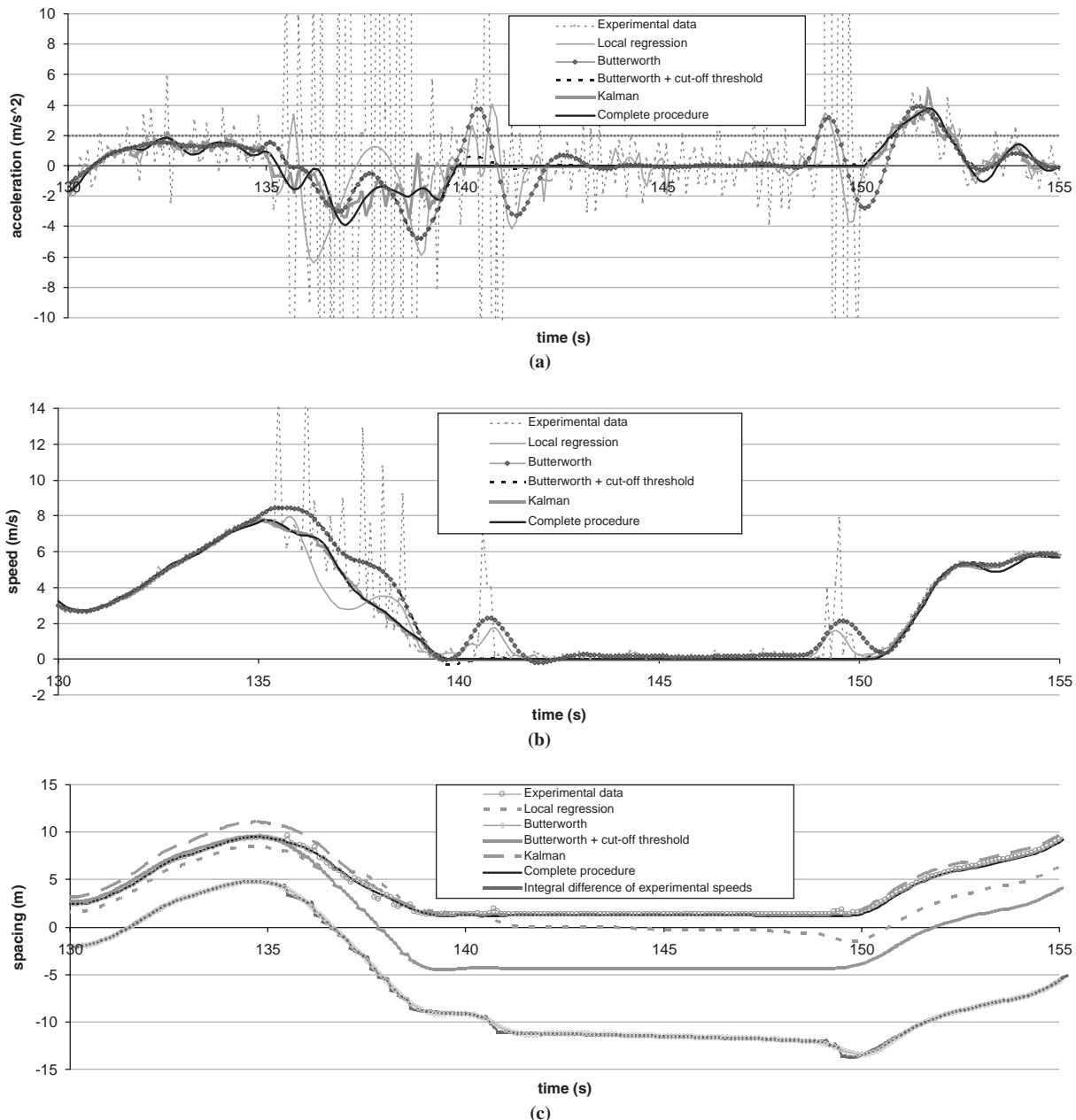

FIGURE 1   Measured and estimated (a) accelerations, (b) speeds, and (c) intervehicle spacings from Experiment 25B.

elsewhere (*8–10*)], the instability of car-following models can easily arise. This renders such data of no use for model calibration and requires effective data-filtering techniques.

What is expected from such a technique is the reduction of measurement errors. Thus, low-frequency (i.e., smoothed) speed and acceleration profiles in accordance with the human and mechanical responses observed in real phenomena are sought. Moreover, such smoothed profiles must be consistent. In other words, if the estimated speeds of following vehicles n and p, $v_n(\tau)$ and $v_p(\tau)$, respectively, are calculated from the temporal profiles, their intervehicle spacing at time t, $\Delta s_{np}(t)$, is as follows:

$$\Delta s_{np}(t) = \Delta s_{np}(0) + \int_0^t v_n(\tau)d\tau - \int_0^t v_p(\tau)d\tau \qquad \forall t \qquad (1)$$

these values would be expected to be equal to those measured (if the vehicles move in a straight line).

This consistency condition is not at all negligible. Indeed, even slight deviations of estimated speeds from real ones may signify a strong deviation of the estimated phenomenon from the real one. Figure 2 clarifies this aspect: the real speed profiles of two following vehicles (measured on the left scale) are reported as dark thick and thin lines (V1 biased and V2 unbiased respectively), while their intervehicle spacings (measured on the right scale) are reported as a light line (Δs12 unbiased). When the speed of the lead vehicle is higher than that of the following vehicle, i.e., vehicles are accelerating and the dark thick line stays above the dark thin one, the intervehicle spacing increases by a quantity measured by Equation 1 and is represented by the light-colored areas. By contrast, when the vehicles decelerate, their space headway decreases by an amount equal to the dark areas. If one estimates for the following vehicle (the dark thin one) a speed profile (V2 biased) that deviates by a quantity equal to the area with vertical lines, the resulting intervehicle spacing would be represented by the light dotted line (Δs12 biased). If a speed profile that deviates by a quantity equal to the area with vertical lines is estimated for the following vehicle (represented by the dark thin line), the resulting intervehicle spacing would be represented by the light dotted line (instead of the light one). Figure 2 therefore shows how even slight and short-lasting errors (4 s in the example) in the estimation of speeds may give rise to an integral error that cannot be further remedied. To

have an idea of the magnitudes involved, consider the case in which vehicle positions are measured every 0.1 s, which is the time step generally used in simulation. If data are not filtered, the same sign measurement errors of only 10 cm for 2 s give rise to an error of 2 m in traveled space. When vehicles have stopped and are presumably 1 m apart, this might entail a negative spacing between the vehicles.

Data Collection Techniques

Two different approaches are suitable for the collection of car-following data. The first makes use of remote sensing and object tracking from video cameras. The second envisages the use of instrumented vehicles.

In the first approach, cameras either can be mounted at fixed and preferably elevated locations (*11*) or can be movable by attachment to aerial platforms (*12, 13*). This approach allows the collection of a large number of trajectories, but only along a limited stretch of road (rarely up to 500 m). Car-following, lane-changing, and gap acceptance behaviors are observable. Moreover, traffic flow is not disturbed at all. However, the observation and analysis of driving behavior can be affected by spatial limitation. Multiple-camera stitching is a possible solution, yet it is far from straightforward. The experimental setup and data processing are time-consuming. Accuracy ranges from 10 to 100 cm, and the detection rate ranges from 80% to 98% (*11*).

Among the techniques used for the second approach, one has recently proved to be successful (*14*). It consists of equipping a vehicle with at least two types of instruments: a speed sensor (e.g., a laser speedometer) and a relative spacing and speed sensor (e.g., a radar). This technique allows the trajectory of a following vehicle, unaware of the experiment, to be monitored for long stretches along a route. Thus, it provides, on the one hand, the opportunity to capture a driver's behavior under variable environmental and traffic conditions; on the other hand, it restricts the analysis to the car-following dynamics of a single pair of vehicles. Radar accuracies, for example, are ±0.2 m in range and ±0.4 m/s in relative speed (*14*).

An alternative methodology follows the development of GPSs: by equipping all the vehicles of a platoon with receivers and monitoring their trajectories, advances can be made in understanding driving behavior, as in this way the internal dynamics of a whole platoon can be thoroughly analyzed [see the report of an experiment
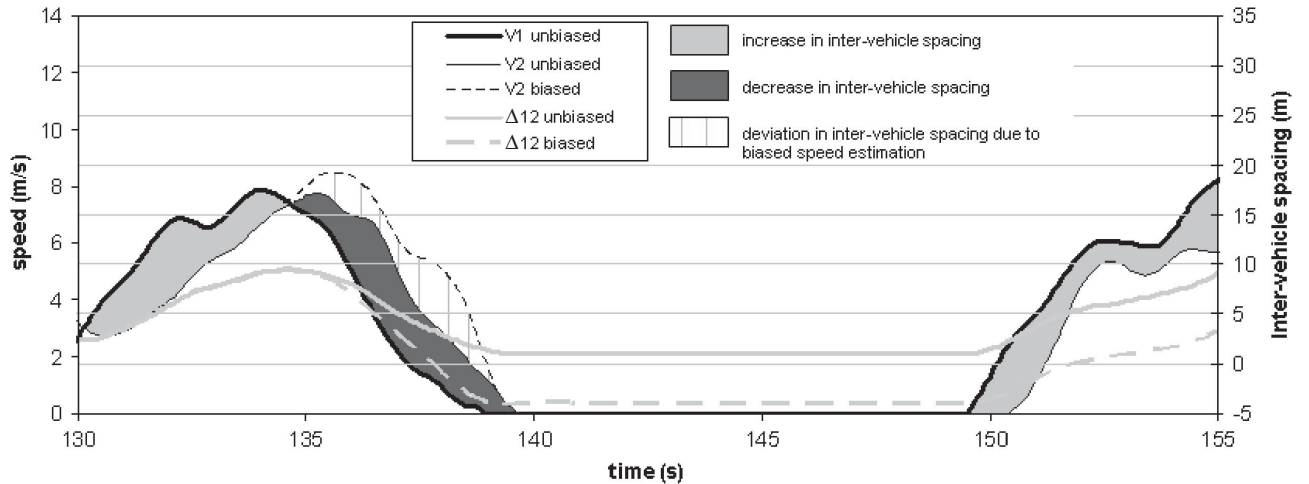

FIGURE 2   Biased and unbiased speeds (intervehicle spacings) for Vehicle 1 (V1) and Vehicle 2 (V2).

carried out with 10 vehicles along a Japanese motor racing track (*6*)]. GPS can effectively support this kind of experiment because of three characteristics peculiar to the system:

- Accuracy in the detection of positions, which, in the case of differential correction on signal carriers, reaches an expected value of approximately 10 mm;
- Thorough timing of the system, which allows synchronous detection of vehicle positions; and
- Sampling frequency of measurements (up to 20 Hz), which is higher than that of the usual simulation steps adopted.

As the techniques described above are limited to car-following behavior, if information on the surrounding traffic is required, additional data collection systems must be used. The drawback is that drivers are aware that they are participating in experiments; besides, if the latter technique is performed in real traffic, unexpected events (e.g., the intrusion of a nonmonitored vehicle into the platoon) can invalidate the test. The latter can be mitigated by the adoption of appropriate countermeasures, as described below.

At present, none of the available techniques seems to be definitively better than the others, with each having a preferential field of application. For example, studies aimed at comparison of the abilities of car-following models to reproduce real behaviors need trajectories from the same driver faced with different types of roads and traffic conditions. Indeed, model performance as well as the optimal parameters calibrated varies for the same driver under different driving conditions (*10*). For this reason and despite its drawbacks, the GPS approach seems to be a good compromise for the collection of such data.

Collected Experimental Data

An experiment similar to that carried out on a test track in Japan (*6*) was performed under real traffic conditions along roads in areas around Naples, Italy, in 2002 and 2003. The trajectories of four vehicles in a platoon were collected both on urban and on Sextraurban roads with GPS devices. The latter consisted of five dual-frequency, GPS + Global Navigation Satellite System receivers (one base station receiver and four rovers) with the following expected precision in real-time kinematic mode: horizontal = 10 mm + 1.0 ppm; vertical = 15 mm + 1.0 ppm. The measurements obtained from the receivers are discussed in the next section.

The aim of the experimental survey was to collect car-following data for multiple cars under different real driving conditions (i.e., on different roads and under different traffic conditions) to be used for comparison of the car-following models. The choice of roads was crucial: several trials were performed on different types of roads. In this work and in the subsequent study of model comparison (*10*), only data for one-carriageway roads with one lane per direction (urban and rural) were analyzed. On such roads, car-following behavior is unaffected by lane-changing behavior.

Data were collected on two days (October 30, 2002, and February 25, 2003) along the same route and consist of five data sets (Experiments 30A, 30B, 30C, 25B, and 25C, respectively) that altogether amount to ca. 24 min. The data sets from October 30 were collected on both urban roads (Experiments 30A and 30C) and a rural road (Experiment 30B). The data sets from February 25 were gathered on the same urban roads from which the data were collected in October. Figure 3 shows maps of the GPS tracks of the trials (tracks on the same road have been translated so that they are observable).

The first urban road, Via Terracina (Experiments 30C and 25B), is a straight road ca. 2 km long that departs from the Naples Engineering Faculty and that heads toward the suburb of Agnano; it has four intersections (two of which are signalized). It is often congested because of the presence of stores, a hospital, a school, and parking places on both sides of the road [the estimated capacity is 900 vehicles per hour (veh/h)]. Data for this road were collected under conditions congested traffic (i.e., stop-and-go traffic conditions) in both October and February.

The second urban road, Via Cinthia (Experiments 30A and 25C), is a straight road approximately 2 km long that departs from the Naples Engineering Faculty and that heads toward the suburb of Soccavo. It has one signalized intersection and terminates with a roundabout. It does not have as many lateral disturbances as Via Terracina and has no parking places (the estimated capacity is 1,200 veh/h). Data for this road were collected under congested traffic conditions in both October and February.

The rural road (Experiment 30B) is a two-lane highway that bypasses the historical center of Pozzuoli, not far from the first two sites. It is approximately 3 km long and has two intersections (one signalized). It has no lateral access, and its estimated capacity is 1,500 veh/h. The traffic flow at the time that the data were gathered was approximately 400 veh/h.

Careful attention was paid to the setup of the experimental protocol. The leader of the platoon was one of the authors. The following drivers, all of them university students, were informed of the path to be taken and were familiar with it, but they were unaware of the aim of the experiment. The leader took care to prevent intrusions into the platoon by giving way to extraneous vehicles at intersections. When intrusions occurred, the corresponding data were discarded.

Initial data analysis highlighted a level of noise higher than that in previous investigations (*6*) because of the environmental conditions of experiments performed in an urban environment with disturbed measurement signals (electromagnetic interference or physical obstacles to the satellite signal) and multipath effects.

MEASUREMENTS FROM GPS DEVICES

Available Measures

GPS allows the position of a receiver to be estimated in Cartesian coordinates, *x, y,* and *z,* in the Word Geodetic System 84 reference system. As mentioned above, time series of intervehicle spacings are immediately available from position data. Indeed, given the synchrony of measurements among the GPS receivers, it is possible to obtain the observed intervehicle spacing in instant t_k, $\Delta s_{np}^{obs}(t_k)$, between the receiver antennas on two vehicles, *n* and *p,* as the distance between their positions at t_k:

$$\Delta s_{np}^{obs}(t_k) = \sqrt{\begin{aligned}&[x^n(t_k) - x^p(t_k)]^2 + [y^n(t_k) - y^p(t_k)]^2 \\ &\quad + [z^n(t_k) - z^p(t_k)]^2\end{aligned}} \qquad (2)$$

where $[x^n(t_k), y^n(t_k), z^n(t_k)]$ are the coordinates of vehicle *n* at instant t_k, and $[x^p(t_k), y^p(t_k), z^p(t_k)]$ are the coordinates of vehicle *p* at instant t_k.

By considering the positions of a vehicle in two successive measurement instants, it is possible to calculate the space traveled in the sampling interval. The length of the space, *T,* is constant and is equal to 0.1 s in this work.

The average observed speed, $v_n^{obs}(k)$, of vehicle *n* in interval *k* between consecutive measurement instants t_{k-1} and t_k is equal to the ratio between the space traveled in *k* and the length *T:*
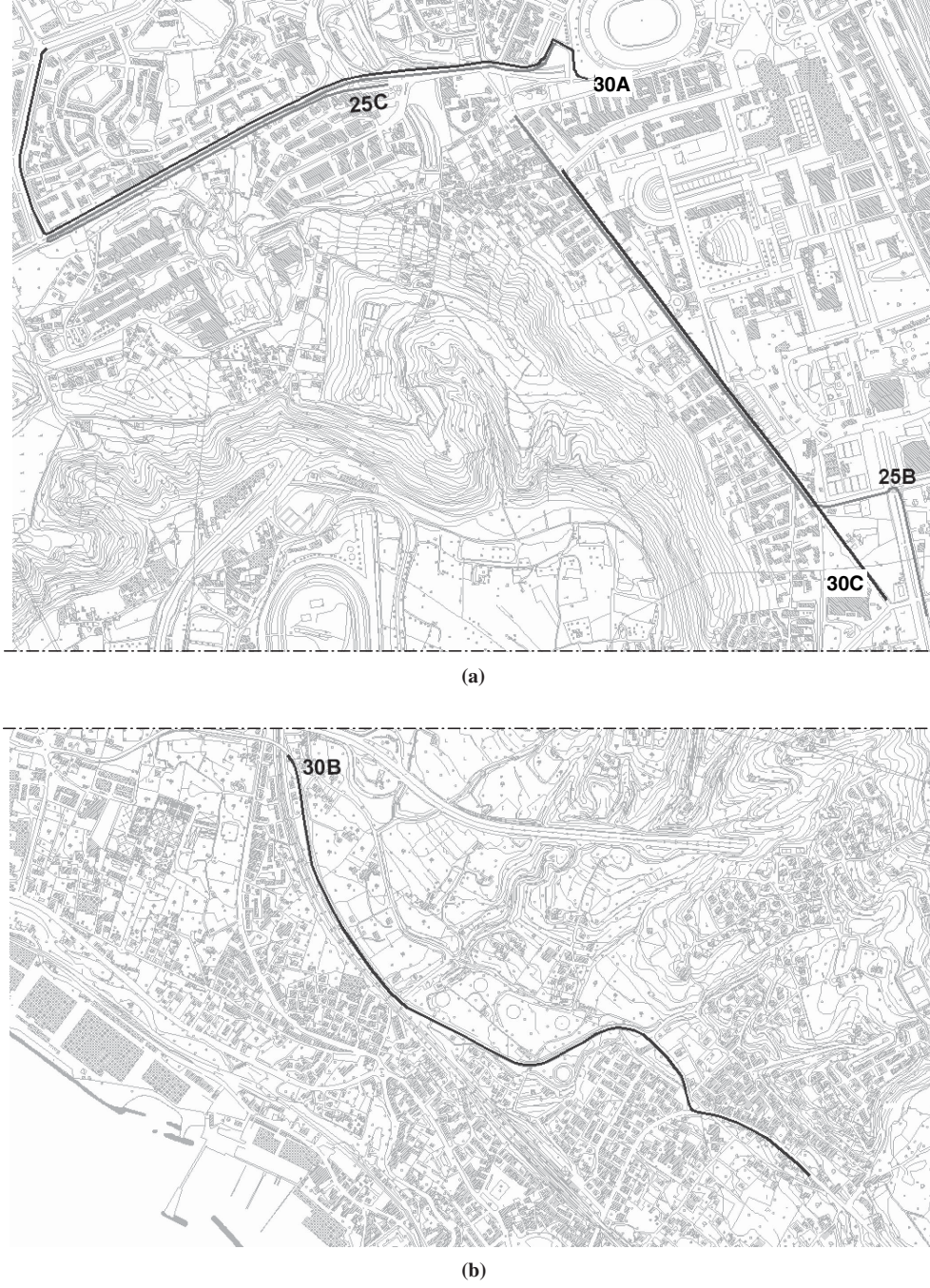
(a)

(b)

FIGURE 3   Data collection sites.

$$v_n^{\text{obs}}(k) = \frac{\sqrt{\begin{array}{c}\left[x^n(t_k) - x^n(t_{k-1})\right]^2 + \left[y^n(t_k) - y^n(t_{k-1})\right]^2 \\ + \left[z^n(t_k) - z^n(t_{k-1})\right]^2\end{array}}}{T} \qquad (3)$$

where $[x^n(t_k), y^n(t_k), z^n(t_k)]$ are the coordinates of vehicle n at instant t_k, and $[x^n(t_{k-1}), y^n(t_{k-1}), z^n(t_{k-1})]$ are the coordinates of the vehicle n at instant t_{k-1}.

The deviation from reality consists of mistaking the space actually traveled by the vehicle during interval k with the straight space between the start and end positions in that interval. This error appears to be negligible when the sampling frequency (10 Hz) is considered.

Intervehicle spacing Δs_{np} at instant t_k either can be measured directly from the positions at t_k through Equation 2 or can be calculated by the integral relation in Equation 1, with v_n and v_p measured from time zero to t_k, through Equation 3. In the first case, the deviation from the true value depends on the measurement errors at the sole instant t_k. In the second case, the deviation is affected by all the measurement errors in interval $[0, t_k]$ (with the two values being equal only for consistent speeds). Hence, unlike speeds, the measured intervehicle spacings are suitable as reference measurements in the estimation process, as

they are memoryless measurements. In conclusion, the available data are (*a*) the time series of the instantaneous intervehicle spacings at intervals of 0.1 s for each pair of vehicles and (*b*) the time series of average speeds in intervals of 0.1 s for each vehicle.

Propagation of Uncertainties in Differential GPS Measurements

GPS also provides an estimate of uncertainty in the measurement of each coordinate by providing its mean square error. From the latter it is possible to calculate how error propagates into intervehicle spacings and speed measurements. Awareness of such errors is essential for the implementation of a Kalman filter.

In the GPS surveys carried out, estimate of the error at each measurement instant (epoch) was obtained by solving the so-called differential problem. By this technique, data from mobile stations were correlated with those from a reference station and thus provided an accuracy of about 1 cm. Less accurate measurements may be attributed to residual errors due to so-called multipath phenomena, which are quite widespread in the urban context and which result from the duplication of the signal following its reflection on surfaces (e.g., buildings) close to the receivers.

The solution of the differential problem corresponds to the solution of an overdetermined system of linear equations (measurements of coordinates at each epoch) that, when solved by a least-squares technique, returns the information required as a variance–covariance matrix of measures.

This matrix is a generalized diagonal in which each element refers to an epoch, t_k, and is represented by the estimates of measurement covariances of the three coordinates of vehicle n, $[x^n(t_k), y^n(t_k), z^n(t_k)]$, indicated in this section as $[x_1^n(t_k), x_2^n(t_k), x_3^n(t_k)]$:

$$
\begin{bmatrix}
\sigma_{x_{11}}^{n,t_k} & \sigma_{x_{12}}^{n,t_k} & \sigma_{x_{13}}^{n,t_k} \\
\sigma_{x_{21}}^{n,t_k} & \sigma_{x_{22}}^{n,t_k} & \sigma_{x_{23}}^{n,t_k} \\
\sigma_{x_{31}}^{n,t_k} & \sigma_{x_{32}}^{n,t_k} & \sigma_{x_{33}}^{n,t_k}
\end{bmatrix}
$$

where $\sigma_{x_{ij}}^{n,t_k}$ is the compact notation that expresses the covariance of $x_i^n(t_k)$ and $x_j^n(t_k)$, with i and j equal to 1, 2, and 3, for vehicle n at t_k.

In this work only values of variances were available (the boldface elements in the matrix), as they are the only data returned by the software used to solve the differential problem (*15*). From estimates of variances of the 12 starting variables, indicated here by $x_1, x_2, \ldots, x_{12}$ and equal to the coordinates of two vehicles in two successive instants, covariances of the two arriving variables $\Delta s_{np}(x_1, x_2, \ldots, x_{12})$ and $v_n(x_1, x_2, \ldots, x_{12})$ were obtained; and these are equal to the intervehicle spacing and the speeds, respectively, of the two vehicles given in Equations 2 and 3.

In the case of small errors, by linearizing the functions $\Delta s_{np}(x_1, x_2, \ldots, x_{12})$ and $v_n(x_1, x_2, \ldots, x_{12})$ around the expected values with the notations adopted, the following formula, which expresses the propagation of variances and covariances in a compact form, is obtained:

$$
\sigma_{v_n \Delta s_{np}} = \sum_{i,j} \frac{\partial v_n}{\partial x_i} \frac{\partial \Delta s_{np}}{\partial x_j} \sigma_{x_{ij}}
\tag{4}
$$

where $\sigma_{v_n \Delta s_{np}}$ and $\sigma_{x_{ij}}$ are the covariances of Δs_{np} and v_n and of x_i and x_j, respectively.

By expressing the derivatives in Equation 4 at the finite differences and by developing relative calculations, the required variances (Var) and covariances (Cov) were obtained:

$$
\text{Var}[\Delta s_{np}(k)] = \sigma_{\Delta s_{np}\Delta s_{np}}
$$

$$
= \sum_{i=1}^{3}\left[\frac{x_i^n(t_{k-1}) - x_i^p(t_{k-1})}{\Delta s_{np}(k)}\right]^2 \left[\sigma_{x_{ii}}^{n,t_{k-1}} + \sigma_{x_{ii}}^{p,t_{k-1}}\right]
\tag{5}
$$

$$
\text{Var}[v_n(k)] = \sigma_{v_n v_n}
$$

$$
= \sum_{i=1}^{3}\left[100\,\frac{x_i^n(t_k) - x_i^n(t_{k-1})}{v_n(k)}\right]^2 \left[\sigma_{x_{ii}}^{n,t_k} + \sigma_{x_{ii}}^{n,t_{k-1}}\right]
\tag{6}
$$

$$
\text{Cov}[v_n(k), \Delta s_{np}(k)] = \sigma_{v_n \Delta s_{np}}
$$

$$
= \sum_{i=1}^{3}\left[-100\,\frac{x_i^n(t_k) - x_i^n(t_{k-1})}{v_n(k)}\right]
$$

$$
\cdot\left[-\frac{x_i^n(t_{k-1}) - x_i^p(t_{k-1})}{\Delta s_{np}(k)}\right] \cdot \sigma_{x_{ii}}^{n,t_{k-1}}
\tag{7}
$$

where $\sigma_{\Delta s_{np}\Delta s_{np}}$, $\sigma_{v_n v_n}$ and $\sigma_{v_n \Delta s_{np}}$ are, respectively, the variances of Δs_{np} and v_n and the covariance of v_n and Δs_{np}, expressed in the compact form by Equation 4, and where $\Delta s_{np}(k)$ indicates the intervehicle spacing of vehicles n and p in period of time k, which is understood to be equal to the spacing calculated in the initial instant of this time period as given by Equation 2 $[\Delta s_{np}(k) = \Delta s_{np}(t_{k-1})]$. Thus, the notation that will prove useful in specifying the Kalman filter has been introduced.

DATA FILTERING PROBLEM

The following were used to filter the data:

- Local regression techniques,
- Selective filters (low-pass filters), and
- Kalman filters.

The first two techniques filter the trajectories of different vehicles one at a time. Hence, they can estimate inconsistent speeds (as described above).

Local Regression Technique

The first technique tested was a local regression technique (*16*), which was enhanced with a preliminary cutoff threshold on measurement errors. It is widely used instead of regular regression estimates when data that require a flexible functional form, as in the case of time series data over traveled space, are being evaluated (*5*).

It processes the coordinates of each single receiver, which were previously subjected to a differential correction, and returns the sequence of instantaneous speeds in instants of measurement sampling (each 0.1 s).

The main steps of the procedure are

1. Elimination of data with an error estimated downstream of a differential correlation over a predefined threshold;

2. Interpolation of missing data with a cubic spline;
3. Calculation of the curvilinear abscissa from the positions;
4. Search for the best polynomial interpolator by least-squares analysis for a window of points of predefined width (local regression);
5. Calculation of the first and second derivatives in the central point of the window (instantaneous speed and acceleration);
6. Repeat of Steps 4 and 5 until speed and acceleration are within the constraints; and
7. Repeat of Steps 4 to 6 for all the points of the vector of the curvilinear abscissas.

This procedure makes it possible to smooth the speed profiles when the signals are not greatly disturbed. Yet, it has two clear drawbacks: (*a*) uncertainty in the choice of parameters of local regression and of the threshold applied and (*b*) inconsistent estimation of vehicle speeds.

Selective Filters

The second technique consisted of the application of low-pass selective filters [e.g., as in a study described previously (*8*), which used a Savitzky–Golay filter to estimate accelerations] and, in particular, a fourth-order Butterworth filter. Spectrum analysis did not allow clear identification of the cutoff frequency, which was therefore obtained by simulation (and which was equal to 0.5 Hz).

Qualitative analysis of the results can be summed up as follows:

• With observed speeds slower than ca. 0.3 m/s (when the vehicle is presumably still), the noise is in the same band as the GPS signal and is not cut off by the filter. The problem, however, can be solved by setting zero speeds equal to these values before application of the filter; and
• With observed speeds higher than ca. 0.3 m/s (running conditions), the noise usually has frequencies higher than those of the GPS signal and is eliminated by the filter.

However, a polarized noise of the measured signal, probably caused by multipath phenomena, was sometimes observed. In this case, although the filter eliminated the high frequency in the signal, it gave back an inconsistent estimate. A clear example of this is reported in Figure 1 (Vehicle 2), for which the noisy signal detected is indicated as "Experimental data," the filter response is indicated as "Butterworth," and the unbiased estimate is indicated as "Complete procedure." The effects of this biased filtering on the consistency of speeds are presented in Figure 2 and were discussed in the section on the requirements of the experimental data.

Kalman Filter

The Kalman filter is a linear device that allows estimation with the minimum mean square error (*7*). In the formulation of the problem, it is first necessary to develop the system state equations concerned and the measurement equations, which are expressed as follows, respectively:

$$x(k + 1) = A(k) \cdot x(k) + B(k) \cdot u(k) + D(k) \cdot \gamma(k)$$

$$y(k) = C(k) \cdot x(k) + \zeta(k)$$

where

$x(k)$, $u(k)$, and $y(k)$ = the variables of state, input, and output, respectively, at instant k;
$\gamma(k)$ and $\zeta(k)$ = errors due to the model and to the measurements, respectively; and
$A(k)$, $B(k)$, $C(k)$, and $D(k)$ = matrices of the coefficients of the variables of state, input, measurements, and errors due to the model, respectively, which are generally variable with the instant k.

Errors (E) due to the model and errors of measurement are white stochastic processes with zero mean and known covariance matrix

$$E[\gamma(k)] = 0 \qquad E[\zeta(k)] = 0$$

$$E[\gamma(k_i)\gamma(k_j)^T] = Q(k_i)\delta_{ij} \qquad E[\zeta(k_i)\zeta(k_j)^T] = R(k_i)\delta_{ij}$$

where

δ_{ij} = Kronecker symbol,
$Q(k_i)$ = covariance matrix of system noise $\gamma(k)$, and
$R(k_i)$ = covariance matrix of measurement noise $\zeta(k)$.

$Q(k_i)$, which is greater than or equal to 0, and $R(k_i)$, which is greater than or equal to 0, are known; δ_{ij} is equal to 0 for i not equal to j; and δ_{ij} is equal to 1 for i equal to j.

The filter estimates $[\hat{x}_F(k)]$ are obtained by solving the following equation:

$$\hat{x}_F(k) = \hat{x}_P(k) + K(k) \cdot [y(k) - C(k) \cdot \hat{x}_P(k)]$$

where $\hat{x}_P$ is the one-step prediction at k, obtained by solving the following recursive equation:

$$\hat{x}_p(k) = A(k - 1) \cdot \hat{x}_F(k - 1) + B(k - 1) \cdot u(k - 1)$$

The matrix $K(k)$ is called the gain matrix:

$$K(k) = P_p(k) \cdot C(k)^T \cdot [C(k) \cdot P_p(k) \cdot C(k)^T + R(k)]^{-1}$$

and represents a compromise between two distinct requirements. These two requirements are the need to use the available measurements to adjust the model estimate of the future state and the need not to downgrade this estimate because of errors in measurements. The gain matrix is proportional to the covariance matrix of the estimate error, $P_P(k)$, which must be updated for every step through the following formula:

$$P_p(k + 1) = A(k) \cdot P_F(k) \cdot A(k)^T + D(k) \cdot Q(k) \cdot D(k)^T$$

where $P_F(k)$ is given by

$$P_F(k) = [I - K(k) \cdot C(k)] \cdot P_p(k)$$

where I is the unit matrix.

KALMAN FILTER DESIGNED

As described in the section above, the Kalman filter, compared with the techniques tested previously, provides the opportunity to implement a model of the system concerned. The response of such a model

is thus adjusted through the available measurements, the weights of which are proportional to the quality of the measurements themselves as well as to the accuracy of the model.

The filter was therefore devised to jointly use speed measurements for n vehicles and the measurements of the $n-1$ intervehicle spacings by constraining the integral differences of the estimates of the former to be equal to the latter. The problem is presented below in relation to just two vehicles, as the extension of the case to n vehicles is trivial. The following were assumed as state variables:

$v_1(k)$ = speed of vehicle 1 in k (space traveled in k divided by T);
$v_2(k)$ = speed of vehicle 2 in k (space traveled in k divided by T); and
$\Delta s_{12}(k)$ = intervehicle spacing of vehicles 1 and 2 in k (i.e., in the initial instant of k, t_{k-1}).

As measurements, values of $v_1^{\text{obs}}(k)$, $v_2^{\text{obs}}(k)$, and $\Delta s_{12}^{\text{obs}}(k)$ are given by Equations 3 and 2.

The state equations and output equations were as follows:

$$\begin{cases} v_1(k+1) = v_1(k) + \gamma_1 \\ v_2(k+1) = v_2(k) + \gamma_2 \\ \Delta s_{12}(k+1) = \Delta s_{12}(k) + [v_1(k) - v_2(k)]T + \gamma_3 \end{cases} \quad \begin{cases} v_1^{\text{obs}}(k) = v_1(k) + \zeta_{11}(k) \\ v_2^{\text{obs}}(k) = v_2(k) + \zeta_{22}(k) \\ \Delta s_{12}^{\text{obs}}(k) = \Delta s_{12}(k) + \zeta_{33}(k) \end{cases}$$

where stationary matrices A, B, C, and D are equal to

$$A = \begin{bmatrix} 1 & 0 & 0 \\ 0 & 1 & 0 \\ T & -T & 1 \end{bmatrix}$$

$$B = [\mathbf{0}]$$

$$C = \begin{bmatrix} 1 & 0 & 0 \\ 0 & 1 & 0 \\ 0 & 0 & 1 \end{bmatrix}$$

$$D = \begin{bmatrix} 1 & 0 & 0 \\ 0 & 1 & 0 \\ 0 & 0 & 1 \end{bmatrix}$$

Evolution of the two state variables $v_1(k)$ and $v_2(k)$ is described by a random walk, in which γ_1 and γ_2 are parameters to be calibrated (together with γ_3). The measuring errors, ζ_{ii} with i meaning 1, 2, 3, instead, are evaluated as mean square errors from the variances in Equations 5 and 6. These variances, together with the variance from Equation 7, make it possible to work out the covariance matrix of errors $R(k)$:

$$R(k) = \begin{bmatrix} \sigma_{v_1(k),v_1(k)} & 0 & \sigma_{v_1(k),\Delta s_{12}(k)} \\ 0 & \sigma_{v_2(k),v_2(k)} & \sigma_{v_2(k),\Delta s_{12}(k)} \\ \sigma_{\Delta s_{12}(k),v_1(k)} & \sigma_{\Delta s_{12}(k),v_2(k)} & \sigma_{\Delta s_{12}(k),\Delta s_{12}(k)} \end{bmatrix}$$

Filter initialization occurs by requiring $\hat{x}_p(k_0)$ to coincide with the measurement vector of v_1, v_2, and Δs in the initial instant and by requiring the covariance matrix $P_P(k_0)$ to be the identity matrix.

The filter is suitable for application to time series of position data, regardless of the technique used to collect data. If such a technique provides time-varying information on measurement errors (as for GPS data after differential correction), the nonstationary filter designed here can be adopted. Otherwise, the stationary counterpart of the filter can be applied by fixing a time-independent covariance matrix of errors R (e.g., data from video cameras).

The availability of a system model represented by n vehicles of the platoon appears to be particularly useful for the case concerned. Estimation of the trajectory of a generic vehicle does not depend exclusively on the single measurements obtained for that vehicle but is bound to the observance of the overall dynamics of the system. This allows consistent estimates of the speed profiles of the vehicles in a platoon to be obtained, which is a fundamental requirement of data for car-following studies. The filter formulation shows that the estimate of the speed of a vehicle directly depends on the measurements obtained for the vehicle itself, as well as on the measurements obtained for the two adjacent vehicles and, through the latter, the measurements obtained for all other vehicles in the platoon.

The adoption of a state equation that deals with intervehicle spacings makes it possible to use the dynamic filter. The system of equations describing the motion of a single vehicle for which only positioning measurements are known is not observable, and its observability matrix (i.e., $[C, CA, \ldots, CA^{n-1}]^T$) is not of maximum rank. Hence, estimation of its speed profile through the use of a dynamic filter will require an additional measurement (e.g., when dealing with a vehicle instrumented with GPS, this is generally accomplished by means of additional sensors, such as odometers and accelerometers). By considering instead n vehicles simultaneously, it is possible to include in the system an additional measurement (intervehicle spacings) that makes the system observable.

Some further considerations concern filter stability. From the equations presented above, it is easy to obtain the model of the estimation error (e):

$$e(k+1) = \{A - [K(k) \cdot C]\} \cdot e(k)$$

If the gain matrix K is constant (i.e., the filter is stationary), the filter is stable if and only if eigenvalues of process matrix $E = (A - K \cdot C)$, are less than 1, that is, if $D \cdot Q \cdot D^T$ is definitely positive. In other words, the appropriate setting of the model error matrix Q makes the filter stable. Unlike stationary filters, results of the stability of time-varying filters tend to be complex; e.g., the condition applied above to E for any k becomes necessary [sufficient conditions are also described elsewhere (17)]. From a practical point of view, the training of the filter with different matrices Q can overcome instability effects.

Note, in conclusion, that to avoid filter estimation of negative or small, nonnull speed values on vehicle stopping, some conditions were added to ease the convergence toward null values.

FURTHER REFINEMENT TO ESTIMATES

As mentioned above, the Kalman filter finds a compromise between measurements and model estimates. Thus, the estimates obtained are not necessarily strictly consistent; i.e., they do not strictly observe state equations of the system. In other words, the intervehicle spacings calculated from estimated speeds can differ slightly from the intervehicle spacings given as output by the filter itself. This is because the assumption that γ_3 is not equal to 0 turns out to be necessary. Indeed,

vehicles move in the three-dimensional space (and the GPS measurements are three-dimensional as well); hence, Equations 2 and 3 cannot verify exactly the third state equation unless both vehicles are moving exactly on the same line in the three-dimensional space. Anyhow, if this consistency were ensured, the following constrained optimization problem could be stated: to find the values of speeds that are as close as possible to the Kalman estimates and that strictly respect true intervehicle spacings (as "true" intervehicle spacings, Kalman filter estimates can be assumed). In mathematical terms

$$\min_{v_1 v_2} \gamma = [v_1(k) - \hat{v}_1(k)]^2 + [v_2(k) - \hat{v}_2(k)]^2 \qquad (8)$$

subject to

$$\Delta s_{12}(k+1) = \Delta s_{12}(k) + [v_1(k) - v_2(k)]T$$

where v_1 and v_2 are the Kalman filter estimates of the speeds.

A closed solution can be obtained by the Lagrange multipliers method.

RESULTS AND COMPARISONS

To compare qualitatively the various techniques applied to the same data, note the results illustrated in Figure 1. The data were chosen for their relevance to the study concerned and show strong noise with polarization of the measurement signal for a length of about 4 s (multipath phenomena in measurements from seconds 135 to 139). They are a sample from the trajectory of the second vehicle of the platoon in data set 25B. The techniques compared were as follows: a local regression procedure, a Butterworth filter, a Butterworth filter with a cutoff threshold on speeds of less than 0.3 m/s, the Kalman filter, and the complete procedure (i.e., the Kalman filter, the consistency problem, and the Butterworth filter).

Figure 1 reports the acceleration and speed profiles of the second vehicle of the platoon and the intervehicle spacing profile between the first and second vehicles as measured and filtered.

The speed profile in the noisy section (between seconds 135 and 139) shows that the local regression procedure almost eliminates all measurements as very noisy (i.e., error estimates are above the threshold), and the resulting profile is the outcome of the cubic spline between points not rejected in the margin of this section. By contrast, the Butterworth filters have a very regular profile, although they are affected by the polarization of the signal: the filtered profile seems to be above the actual profile (which is easy to infer from the observations of experimental data) and is dragged upward by the higher values. Finally, the Kalman filter presents a profile that appears to be the closest to the actual profile.

Figure 1 also presents a comparison of intervehicle spacings. In Figure 1 the measured intervehicle spacing at any instant is given by Equation 2. As mentioned above, this measurement does not depend on those measurements affected in other instants. Moreover, these memoryless errors, which usually amount to some centimeters, have a low percent incidence on intervehicle spacings, which generally amount to some meters. This implies that the intervehicle spacing profile appears to be quite regular, even when the measurements are noisy.

Instead, all profiles obtained with the filtering techniques tested are obtained as differences of integrals of the speeds estimated through these techniques, as speed consistency needs to be checked (and are calculated from instant 0). Therefore, the Kalman label does not indicate the intervehicle spacing estimate made by the filter but, rather, the spacing calculated as the difference of the integrals of speeds estimated by the filter itself. Indeed, these profiles do not always coincide (see the section on further refinement of the estimates).

Figure 1 shows that the only speed estimates that produce an intervehicle spacing consistent with the actual one are those obtained through the Kalman filter. The estimates farthest from the reference measurements are those concerning the spacing calculated on the basis of raw speed measurements and by the speeds filtered through the Butterworth filter. The two profiles coincide as expected, as the latter does not alter the integral of the filtered speeds.

In conclusion, Figure 1 shows the acceleration profiles calculated as the derivative of the estimated speeds as well. In this case the most regular profile appears to be that given by the complete procedure.

Table 1 reports the values of root mean square error (RMSe) and root mean square percentage error (RMSPe) for the intervehicle spacing profiles of all the data sets available in this study. Error test values were computed by comparison of the intervehicle spacings calculated from the speeds estimated by the various techniques and the intervehicle spacings estimated by use of the Kalman filter (which are assumed to be the reference measurements). The results show that the stated problem of the consistency of speeds estimated is not negligible at all. Moreover, only the Kalman filter estimates cover the requirements for the data to be used in car-following studies.

CONCLUSIONS

This study sought to make a contribution to the problem of car-following data collection and estimation. First, the stringent requirements of data for car-following studies were described, highlighting the problem of speed data consistency, i.e., the deviation between the intervehicle spacings calculated from the estimated speed and the true intervehicle spacings. Such a problem arises when the speed profiles of different vehicles are independently estimated from position data (i.e., one at a time).

This problem was tackled by considering vehicles as a sole dynamic system and solving one consistent estimation problem instead of several inconsistent ones. A Kalman filter was designed for this purpose. The filter can be applied to position data regardless of the data collection technique used. The availability of time-varying information on error measurements allowed the design of a nonstationary filter that was applied to five car-following data sets collected by means of a differential GPS.

Adoption of intervehicle spacing as reference measures first allowed the effective design of the filter and then comparison of the performances of the different filtering techniques. The results showed that, unlike the Kalman filter, the techniques that are generally adopted are not suitable for estimation of consistent car-following data. The error that they supply is not at all negligible and makes the data estimated insufficiently accurate for use in car-following studies.

ACKNOWLEDGMENTS

TABLE 1 RMSe and RMSPe Between Intervehicle Spacings Calculated from Estimated Speeds and Intervehicle Spacings Measured

			Local Regression	Butterworth	Butterworth + Threshold	Kalman	Complete Procedure
RMSe [m]	30A	Δs_{12}	3.07	2.73	1.43	0.40	0.24
		Δs_{23}	2.64	2.87	1.62	0.29	0.29
		Δs_{34}	0.77	0.67	0.65	0.22	0.12
	30B	Δs_{12}	1.49	1.34	1.69	0.22	0.27
		Δs_{23}	4.89	0.80	0.80	0.36	0.23
		Δs_{34}	0.85	0.58	0.65	0.25	0.14
	30C	Δs_{12}	4.39	0.84	1.15	0.41	0.11
		Δs_{23}	3.41	4.05	4.99	0.70	0.48
		Δs_{34}	2.73	4.13	3.61	0.46	0.41
	25B	**Δs_{12}**	**1.52**	**7.24**	**2.50**	**0.58**	**0.35**
		Δs_{23}	6.87	10.28	5.58	1.15	0.49
		Δs_{34}	4.11	13.69	7.89	1.57	0.60
	25C	Δs_{12}	1.64	2.43	1.95	1.15	1.17
		Δs_{23}	0.82	2.32	2.33	1.41	0.88
		Δs_{34}	4.40	6.17	3.14	1.41	0.57
RMSPe [%]	30A	Δs_{12}	38.8%	33.1%	16.6%	4.5%	2.6%
		Δs_{23}	29.5%	31.5%	18.4%	3.1%	2.8%
		Δs_{34}	11.7%	11.3%	9.9%	2.3%	1.5%
	30B	Δs_{12}	23.6%	15.6%	19.1%	2.2%	2.9%
		Δs_{23}	43.2%	7.8%	7.8%	2.6%	1.9%
		Δs_{34}	11.6%	8.7%	8.9%	2.6%	1.4%
	30C	Δs_{12}	50.0%	11.0%	14.6%	5.4%	1.5%
		Δs_{23}	33.9%	38.9%	46.9%	6.2%	5.1%
		Δs_{34}	31.1%	45.7%	39.4%	4.3%	3.0%
	25B	**Δs_{12}**	**16.9%**	**85.2%**	**32.0%**	**8.1%**	**4.8%**
		Δs_{23}	65.5%	101.2%	54.3%	12.9%	4.4%
		Δs_{34}	38.9%	133.8%	73.4%	12.2%	6.1%
	25C	Δs_{12}	20.0%	30.6%	23.9%	12.6%	14.0%
		Δs_{23}	8.5%	22.2%	23.2%	14.6%	9.5%
		Δs_{34}	59.8%	86.6%	44.8%	13.7%	8.4%

NOTE: Boldface indicates errors relative to the trajectories found in Figure 3.

REFERENCES

1. Gazis, D. C., R. Herman, and R. W. Rothery. Non-Linear Follow-the-Leader Models of Traffic Flow. *Operations Research,* Vol. 9, 1961, pp. 545–567.
2. Leutzbach, W., and R. Wiedemann. Development and Applications of Traffic Simulation Models at the Karisruhe Institut für Verkehrswesen. *Traffic Engineering and Control,* Vol. 27, No. 5, 1986, pp. 270–278.
3. Gipps, P. G. A Behavioural Car-Following Model for Computer Simulation. *Transportation Research, Part B,* Vol. 15, No. 2, 1981, pp. 105–111.
4. Brackstone, M., and M. McDonald. Car-Following: A Historical Review. *Transportation Research, Part F,* Vol. 2, 1999, pp. 181–196.
5. Ahmed, K. I. *Modeling Drivers' Acceleration and Lane-Changing Behavior.* Ph.D. dissertation. Massachusetts Institute of Technology, Cambridge, 1999.
6. Gurusinghe, G. S., T. Nakatsuji, Y. Azuta, P. Ranjitkar, and Y. Tanaboriboon. Multiple Car-Following Data Using Real-Time Kinematic Global Positioning System. In *Transportation Research Record: Journal of the Transportation Research Board, No. 1802,* Transportation Research Board of the National Academies, Washington, D.C., 2002, pp. 166–180.
7. Anderson, B. D. O., and J. B. Moore. *Optimal Filtering.* Prentice Hall, Inc., Englewood Cliffs, N.J., 1979.
8. Brockfeld, E., R. D. Kühne, and P. Wagner. Calibration and Validation of Microscopic Traffic Flow Models. In *Transportation Research Record: Journal of the Transportation Research Board, No. 1876,* Transportation Research Board of the National Academies, Washington, D.C., 2004, pp. 62–70.
9. Ranjitkar, P., T. Nakatsuji, and M. Asano. Performance Evaluation of Microscopic Traffic Flow Models with Test Track Data. In *Transportation Research Record: Journal of the Transportation Research Board, No. 1876,* Transportation Research Board of the National Academies, Washington, D.C., 2004, pp. 90–100.
10. Punzo, V., and F. Simonelli. Analysis and Comparison of Car-Following Models Using Real Traffic Microscopic Data. Presented at 84th Annual Meeting of the Transportation Research Board, Washington, D.C., 2005.
11. Cambridge Systematics, Inc., Massachusetts Institute of Technology, Siemens ITS, and Dowling Associates. *NGSIM Task E.3: High-Level Data Plan.* Final Report. FHWA, U.S. Department of Transportation, 2004.
12. Hoogendoorn, S. P., H. J. Van Zuylen, M. Schreuder, B. Gorte, and G. Vosselman. *Microscopic Traffic Data Collection by Remote Sensing* (CD-ROM), TRB, National Research Council, Washington, D.C., 2003.
13. Treiterer, J. *Investigation of Traffic Dynamics by Aerial Photogrammetry Techniques.* Final Report EES 278. Transportation Research Center, Department of Civil Engineering, Ohio State University, Columbus, 1975.
14. Brackstone, M., B. Sultan, and M. McDonald. Motorway Driver Behaviour: Studies on Car-Following. *Transportation Research, Part F,* Vol. 5, 2002, pp. 329–344.
15. TOPCON Corp. Pinnacle User's Guide, version 1.0. 1998–2002. www.topcon.com. Accessed September 30, 2002.
16. Cleveland, W. S., S. J. Devlin, and E. Grosse. Regression by Local Fitting, Methods, Properties, and Computational Algorithms. *Journal of Econometrics,* Vol. 37, 1988, pp. 87–114.
17. Amato, F., G. Celentano, and F. Garofalo. New Sufficient Conditions for the Stability of Slowly Varying Linear Systems. *IEEE Transactions on Automatic Control,* Vol. 38, No. 9, 1993, pp. 1,409–1,411.